PROCEEDINGS OF SCIENCE

Constraining self-interacting scalar field dark matter with strong gravitational lensing?

Raquel Galazo García,[a,b,*] **Eric Jullo,**[b] **Emmanuel Nezri**[b] **and Marceau Limousin**[b]

[a] *Universidad Pontificia Comillas,*
C. de Alberto Aguilera, 23, Madrid, Spain
[b] *Aix–Marseille Université, CNRS, CNES, Laboratoire d'Astrophysique de Marseille*
Marseille, France
E-mail: rgalazo@comillas.edu, eric.jullo@lam.fr, emmanuel.nezri@lam.fr, marceau.limousin@lam.fr

We investigate the detectability of soliton cores predicted by self-interacting scalar field dark matter (SI-SFDM) in the Thomas–Fermi regime using strong gravitational lensing by galaxy clusters. We construct semi-analytical density profiles composed of a solitonic core and an outer NFW halo, and compute deflection angles and excess surface mass density for clusters with $M_{200} = 2 \times 10^{15} M_\odot$ and $2 \times 10^{14} M_\odot$. Massive solitons ($\alpha = 3$) generate deflection deviations larger than $2''$ at radii of 10–30 kpc, within the precision of current strong-lensing observations. Comparisons with A2390 and DES weak-lensing measurements show that SI-SFDM remains consistent with large-scale mass profiles while central densities constrain the soliton mass to $M_{\rm sol} \lesssim 10^{12} M_\odot$. Our results indicate that strong lensing provides a promising probe of scalar-field interactions in cluster cores.

The European Physical Society Conference on High Energy Physics (EPS-HEP2025)
7-11 July 2025
Marseille, France

*Speaker

 ISSN 1824-8039 . Published by SISSA Medialab.

PoS(EPS-HEP2025)136

1. Introduction

The cold dark matter (CDM) paradigm successfully explains the large-scale structure of the Universe [1, 2], yet persistent small-scale tensions [3–5]—such as the core–cusp problem and missing satellite problem—motivate the exploration of alternative dark matter models [3, 6]. Scalar field dark matter (SFDM) [7–9], particularly in the ultra-light regime, naturally forms central soliton cores [10–12] arising from the coherent wave-like behaviour of the field. When repulsive self-interactions dominate over quantum pressure, the soliton enters the Thomas–Fermi (TF) regime, leading to a smooth, finite-size core whose properties are independent of the soliton mass [13–16].

Galaxy clusters provide an excellent laboratory to test such deviations from the standard NFW halo structure [17–19]. Strong gravitational lensing (SL) delivers sub-arcsecond constraints on the projected mass distribution in cluster cores, and is therefore sensitive to additional components such as solitons. If a TF soliton contributes non-negligibly to the enclosed mass, it may produce measurable modifications in the deflection field and other SL observables.

In this work, we investigate whether solitons predicted by self-interacting scalar field dark matter (SI-SFDM) produce detectable signatures in strong lensing. We construct semi-analytical halo models combining a TF soliton with an outer NFW profile, and evaluate their impact on deflection angles and excess surface density for cluster-sized halos. We then compare these predictions with observational data, assessing the potential of strong lensing to constrain the soliton parameter space and, more broadly, the self-interaction properties of SI-SFDM.

2. Thomas–Fermi soliton core

In the SI-SFDM model, repulsive quartic interactions dominate over quantum pressure in high-density regions, placing the soliton in the TF regime. The soliton density profile is then fully determined by the interaction scale r_a and the central density ρ_0, and takes the analytic form

$$\rho_{\rm sol}(r) = \rho_0 \, \frac{\sin(\pi r/R_{\rm sol})}{\pi r/R_{\rm sol}}, \tag{1}$$

with soliton radius

$$R_{\rm sol} = \pi r_a, \tag{2}$$

where $r_a^2 = 3\lambda_4/(16\pi G m^4)$ encodes the scalar-field mass m and self-interaction strength λ_4. This profile is valid up to $R_{\rm sol}$, where the soliton sharply transitions to the outer halo.

3. Halo characterization

To model galaxy cluster halos, we assume an inner TF soliton matched to an outer NFW profile [20]:

$$\rho(r) = \begin{cases} \rho_{\rm sol}(r), & r < r_t, \\ \rho_{\rm NFW}(r), & r > r_t, \end{cases} \tag{3}$$

where r_t is the transition radius, defined implicitly by equating the enclosed-mass ratio,

$$M_{\rm sol}(r_t) = \alpha \, M_{\rm NFW}(r_t), \tag{4}$$

with α parametrizing the soliton mass relative to the NFW halo at the point of matching. This approach ensures a physically consistent transition between the dense central soliton core and the more extended NFW halo [21, 22]. The NFW profile is expressed as usual:

$$\rho_{\rm NFW}(r) = \frac{\rho_s}{\frac{r}{r_s}\left(1+\frac{r}{r_s}\right)^2} \tag{5}$$

where ρ_s and r_s are the scale density and scale radius of the halo, respectively. We focus on cluster-scale halos with masses

$$M_{200} = 2\times10^{15}M_\odot \quad \text{and} \quad M_{200} = 2\times10^{14}M_\odot, \tag{6}$$

at lens redshift $z_l = 0.2$, adopting NFW concentrations from [23] with a conservative uncertainty $\Delta c_{200} = \pm1$. For the soliton component, we explore configurations with $\alpha = 1, 3$ and interaction scales $r_a = 5, 15$ kpc, covering a realistic range of TF-soliton masses compatible with cluster-scale halos.

4. Lensing quantities

We compute the two main strong- and weak-lensing observables:

Deflection angle. The azimuthally averaged deflection field [see 24, and references therein] is obtained from the projected surface mass density $\Sigma(r)$ via

$$\hat{\alpha}(r) = \frac{4G}{c^2}\frac{M(<r)}{r}, \tag{7}$$

allowing deviations from the NFW expectation to be quantified.

Excess surface density. We also evaluate the weak-lensing estimator

$$\Delta\Sigma(r) = \Sigma(<r) - \Sigma(r), \tag{8}$$

which characterizes the radial mass contrast and enables comparison with cluster weak-lensing profiles (e.g. [25]). These quantities provide a direct test of how soliton cores modify the projected mass distribution, particularly in the central 10–50 kpc where strong-lensing observables are most sensitive.

5. Results

5.1 Impact of the soliton on density and mass profiles

The analyses in our full paper [26] show that both the soliton mass and its spatial extent increase with the parameters α and r_a. For the massive halo ($M_{200} = 2\times10^{15}M_\odot$), the configuration $\alpha = 3$ and $r_a = 15$ kpc yields a soliton mass of order

$$M_{\rm sol} \sim 10^{13}M_\odot, \tag{9}$$

though its global contribution remains small ($\lesssim 1\%$ of M_{200}). For the lighter halo ($2\times10^{14}M_\odot$), the soliton contributes a larger fraction but still transitions smoothly to the outer NFW profile at a few $\times10$ kpc. In all cases, the soliton produces a noticeable central flattening of the three-dimensional density as showed in Fig.1 and a characteristic bump in the enclosed mass profile.

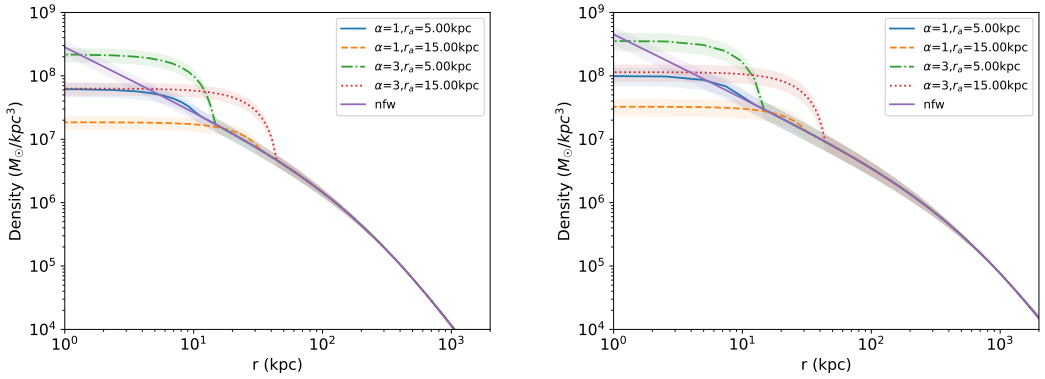

Figure 1: Density profile for different SI-SFDM halos with mass factors $\alpha = 1$ and $\alpha = 3$ and with self-interacting scales $r_a = 5$ kpc and 15 kpc compared with the NFW profile in purple. **Left:** Halo of $M_{200} = 2 \times 10^{14} M_\odot$ **Right:** Halo of $M_{200} = 2 \times 10^{15} M_\odot$.

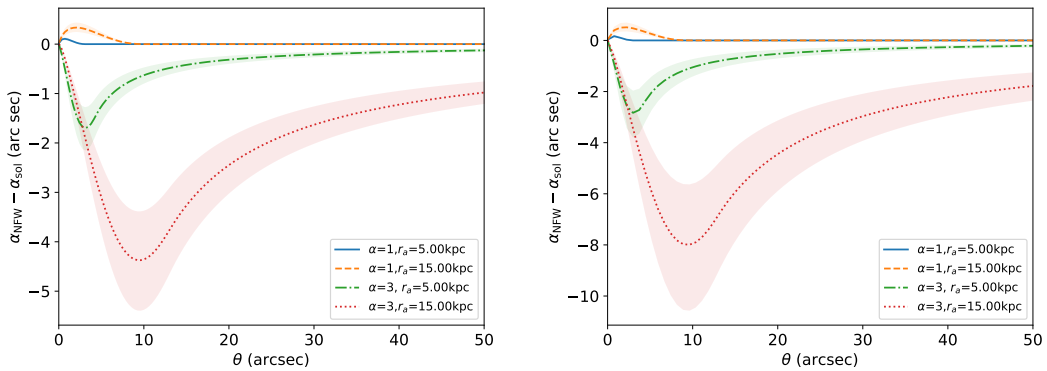

Figure 2: Difference between the deflection angle produced by a NFW halo (CDM) and a soliton+NFW halo (SI-SFDM) for mass factors $\alpha = 1$ and $\alpha = 3$ and for self-interacting scales $r_a = 5$ kpc and 15 kpc. **Left:** Halo of $M_{200} = 2 \times 10^{14} M_\odot$ **Right:** Halo of $M_{200} = 2 \times 10^{15} M_\odot$.

5.2 Deflection angle deviations

A key observable is the deviation of the deflection angle from that of a pure NFW halo, defined as $\Delta\hat{\alpha} = \hat{\alpha}_{\text{sol+NFW}} - \hat{\alpha}_{\text{NFW}}$ and illustrated in Fig. 2. For the $2 \times 10^{15} M_\odot$ halo, we find that a soliton with $\alpha = 3$ and $r_a = 5$ kpc produces deviations exceeding $2''$ at $r \sim 10$ kpc, while the same soliton with $r_a = 15$ kpc produces deviations exceeding $2''$ at $r \sim 31$ kpc. The $2 \times 10^{14} M_\odot$ halo exhibits the same qualitative behavior, with strong deviations ($> 2''$) in the range 10–32 kpc for massive solitons.

Since current strong lensing reconstructions typically achieve precisions $\lesssim 1''$, these deviations are well within observational sensitivity, demonstrating that strong lensing is a powerful probe of soliton cores in the parameter space considered here.

5.3 Comparison with observations

A2390: The galaxy cluster A2390 provides a close observational analog to our most massive simulated halo. Using parameters from combined strong and weak lensing [18], we find that $\alpha = 1$ solitons are consistent with the observed density profile, while $\alpha = 3$ solitons overpredict the central density, yielding a conservative upper limit:

$$M_{\rm sol} \lesssim 10^{12} M_{\odot}. \tag{10}$$

Weak-lensing: We compare our excess surface density $\Delta\Sigma(r)$ with results from [25]. Large-scale profiles ($r \gtrsim 300$ kpc) show excellent agreement for both halos, confirming that SI-SFDM solitons do not affect the mass distribution at large radii. Deviations appear only at $r \lesssim 200$ kpc, where DES data are affected by significant systematics, leaving strong lensing as the main probe of soliton detectability.

Overall, our results show that the expected solitonic modifications occur precisely in the radial range where strong lensing is most sensitive, while remaining consistent with current weak-lensing measurements.

References

[1] G. Jungman, M. Kamionkowski and K. Griest, *Supersymmetric dark matter*, **267** (1996) 195 [hep-ph/9506380].

[2] G. Steigman and M.S. Turner, *Cosmological constraints on the properties of weakly interacting massive particles*, *Nuclear Physics B* **253** (1985) 375.

[3] D.H. Weinberg, J.S. Bullock, F. Governato, R.K. De Naray and A.H. Peter, *Cold dark matter: Controversies on small scales*, *Proceedings of the National Academy of Sciences of the United States of America* **112** (2015) 12249 [1306.0913].

[4] A. Del Popolo and M.L. Delliou, *Small scale problems of the $$CDM model: a short review*, *Galaxies* **5** (2016) [1606.07790].

[5] T. Nakama, J. Chluba and M. Kamionkowski, *Shedding light on the small-scale crisis with CMB spectral distortions*, *Physical Review D* **95** (2017) 121302 [1703.10559].

[6] L. Di Luzio, M. Giannotti, E. Nardi and L. Visinelli, *The landscape of QCD axion models*, *Physics Reports* **870** (2020) 1 [2003.01100].

[7] W. Hu, R. Barkana and A. Gruzinov, *Fuzzy Cold Dark Matter: The Wave Properties of Ultralight Particles*, *Phys. Rev. Lett.* **85** (2000) 1158.

[8] L. Hui, J.P. Ostriker, S. Tremaine and E. Witten, *Ultralight scalars as cosmological dark matter*, **95** (2017) 043541 [1610.08297].

[9] J. Goodman, *Repulsive dark matter*, **5** (2000) 103 [astro-ph/0003018].

[10] T.D. Lee and Y. Pang, *Nontopological solitons*, *Phys. Rept.* **221** (1992) 251.

[11] A.H. Guth, M.P. Hertzberg and C. Prescod-Weinstein, *Do dark matter axions form a condensate with long-range correlation?*, **92** (2015) 103513 [1412.5930].

[12] P. Sikivie and Q. Yang, *Bose-Einstein Condensation of Dark Matter Axions*, **103** (2009) 111301 [0901.1106].

[13] P.-H. Chavanis, *Mass-radius relation of Newtonian self-gravitating Bose-Einstein condensates with short-range interactions: I. Analytical results*, *Phys. Rev. D* **84** (2011) 043531 [1103.2050].

[14] T. Harko, *Evolution of cosmological perturbations in Bose-Einstein condensate dark matter*, *Mon. Not. Roy. Astron. Soc.* **413** (2011) 3095 [1101.3655].

[15] P. Brax, J.A.R. Cembranos and P. Valageas, *Impact of kinetic and potential self-interactions on scalar dark matter*, *Phys. Rev. D* **100** (2019) 023526 [1906.00730].

[16] R. Galazo García, P. Brax and P. Valageas, *Solitons and halos for self-interacting scalar dark matter*, *Physical Review D* **109** (2024) .

[17] D.J. Sand, T. Treu, G.P. Smith and R.S. Ellis, *The Dark Matter Distribution in the Central Regions of Galaxy Clusters: Implications for Cold Dark Matter*, **604** (2004) 88.

[18] A.B. Newman, T. Treu, R.S. Ellis and D.J. Sand, *The density profiles of massive, relaxed galaxy clusters. ii. separating luminous and dark matter in cluster cores*, *The Astrophysical Journal* **765** (2013) 25.

[19] M. Limousin, B. Beauchesne and E. Jullo, *Dark matter in galaxy clusters: Parametric strong-lensing approach*, **664** (2022) A90 [2202.02992].

[20] J.F. Navarro, C.S. Frenk and S.D.M. White, *The Structure of cold dark matter halos*, *Astrophys. J.* **462** (1996) 563 [astro-ph/9508025].

[21] H.Y. Schive, T. Chiueh and T. Broadhurst, *Cosmic structure as the quantum interference of a coherent dark wave*, *Nature Physics* **10** (2014) 496 [1406.6586].

[22] J. Veltmaat, J.C. Niemeyer and B. Schwabe, *Formation and structure of ultralight bosonic dark matter halos*, *Phys. Rev. D* **98** (2018) 043509.

[23] T. Ishiyama, F. Prada, A.A. Klypin, M. Sinha, R.B. Metcalf, E. Jullo et al., *The Uchuu Simulations: Data Release 1 and Dark Matter Halo Concentrations*, *Monthly Notices of the Royal Astronomical Society* **506** (2020) 4210 [2007.14720v3].

[24] M. Bartelmann, *Gravitational lensing*, *Classical and Quantum Gravity* **27** (2010) 233001.

[25] T. McClintock, T.N. Varga, D. Gruen, E. Rozo, E.S. Rykoff, T. Shin et al., *Dark energy survey year 1 results: weak lensing mass calibration of redmapper galaxy clusters*, *Monthly Notices of the Royal Astronomical Society* **482** (2018) 1352–1378.

[26] R.G. García, E. Jullo, E. Nezri and M. Limousin, *Constraining self-interacting scalar field dark matter with strong gravitational lensing in cluster scale?*, 2025.